

OLVASÓTERMI FELDANY

TK 155.149

KFKI-1980-22

H.V. VON GERAMB
G. PÁLLA

ELASTIC AND INELASTIC PROTON SCATTERING
FROM EVEN PALLADIUM ISOTOPES

Hungarian Academy of Sciences

CENTRAL
RESEARCH
INSTITUTE FOR
PHYSICS

BUDAPEST

2017

ELASTIC AND INELASTIC PROTON SCATTERING
FROM EVEN PALLADIUM ISOTOPES

H.V. von Geramb*, G. Pálfa

Central Research Institute for Physics
H-1525 Budapest 114, P.O.B. 49, Hungary

*I. Institut für Experimentalphysik, Universität Hamburg,
Hamburg, West Germany

ABSTRACT

Aspects of scattering experiments from Palladium isotopes are discussed. Five even Pd isotopes are selected to study anharmonicities in the low-lying spectrum. Analysis of the 12 MeV and 52 MeV experimental data taken from the literature is performed by a strong coupling approach. The coupling channel effects with the giant quadrupole resonance are investigated. The complex optical model potential and its local equivalent for ^{110}Pd is evaluated using the complex local Brückner reaction matrices have been calculated from two nucleon potential.

АННОТАЦИЯ

Обсуждаются аспекты экспериментов по рассеянию, проводившиеся с изотопами палладия. Для изучения ангармоничностей, появляющихся при низкоэнергетических возбуждениях, было выбрано пять четных изотопов Pd. Литературные данные по рассеянию протонов с энергией 12 и 52 МэВ были анализированы на моделях с сильной связью. Изучено влияние связи с гигантским квадрупольным резонансом. Для ядра ^{110}Pd рассчитан микроскопический оптический модельный потенциал и его локальный эквивалент из комплексной локальной матрицы реакции, Брюкнера рассчитанной из взаимодействий двух нуклонов.

KIVONAT

Palládium izotópokra vonatkozó szórás kísérlet aspektusait tárgyaljuk. Öt páros Pd izotópot választottunk az alacsonyenergiájú gerjesztéseknél jelentkező anharmonicitások vizsgálatához. Az irodalomból vett 12 és 52 MeV energiájú protonok szórás kísérleti adatait analizáltuk az erős csatolási modellben. Tanulmányoztuk a quadrupól óriás rezonanciával való csatolás hatását. Kiszámítottuk a ^{110}Pd magra a mikroszkópikus optikai modell potenciált és lokális ekvivalensét a lokális komplex Brückner reakciómátrixokból, amelyek a két nukleon kölcsönhatásokból származnak.

1. INTRODUCTION AND OUTLINE

Various proton scattering analyses have been made with the extended optical model and coupled channel approach showing that elastic and inelastic scattering to be a useful tool for structure and reaction mechanism studies. The even palladium isotopes represent a nuclear range where the low lying states display a typical collective vibrational character together with other strong single particle excitations. These series of isotopes $^{102-110}\text{Pd}$, offer an excellent opportunity to investigate the nature of these low energetic excitations as a function of increasing neutron number the $1g_{7/2}$ and $2d_{5/2}$ orbits. Neutron shell closure is reached with ^{110}Pd . Excitations of the proton shell are characterized by arrangements within the $2p_{1/2}$ and $1g_{9/2}$ orbits. An experimentally challenging situation may be seen in high resolution studies of the 2phonon quadrupole multiplets around 1 MeV where the splitting is sometimes only a few keV. Such data enable a detailed study of anharmonicities as they are predicted by a sophisticated multiphonon spectroscopy. The analysis of these results can be made with the extended optical model or with a fully microscopic optical potential for the elastic channel and simply derived transition potentials for inelastic transition form factors. Additionally, a fully antisymmetrized DWBA analysis for the single particle transitions may be considered.

In recent years systematic studies in light to medium weight nuclei have shown that coupling effects with the giant resonances, in particular the GQR, may be of importance. Necessary for this effect is an optical matching condition between relevant partial waves and projectile energies which leave the intermediate state in a quasi closed channel.

The GQR has been studied in the neighbouring Mo nuclei where a strength concentration was observed around $63/A^{1/3}$ (i.e. around 13.5 MeV) with a width of typically 4-5 MeV, exhausting 60-80% of the linear energy weighted sum rule (EWSR) [1]. The same behaviour of the GQR we expect to occur for the Pd isotopes for which no experimental data have become known to us. With the giant resonance region we connect two aspects. The first concerns the GQR structure, isotope dependence, width, strength and other new features of interest. The second concerns the interplay between the giant resonances (here in particular the GQR) and the low lying spectrum with its spectroscopic implications and its reaction mechanism influences.

All these questions cannot be answered in a single experiment at a fixed incident proton energy. We therefore envisage low energy scattering experiments between 15 and 28 MeV at the Hamburg isochronous cyclotron (HAIZY), using a scattering chamber and in the range 40 to 45 MeV at the Jülich isochronous cyclotron (Julic) using the magneticspectrograph (Big Karl). Scattering into the giant resonance region is planned at even higher energies at an alternative institution or with high energetic light ions in Jülich.

The next paragraphs give a theoretical investigation of the above mentioned topics.

2. COUPLED CHANNEL ANALYSIS INVOLVING THE LOW LYING SPECTRUM

Elastic and inelastic proton scattering has been studied in the past at 12 and 13 MeV for $^{106,108}\text{Pd}$ [2] and ^{110}Pd [3]. Angular distribution of elastically and inelastically scattered 12- and 13 MeV protons from ^{106}Pd and ^{108}Pd have been measured for angles between 24° and 165° . Quadrupole and octopole deformation parameters, β_2 and β_3 , were extracted from the experimental cross sections by means of DWBA. The determined values were $\beta_2=0.25$, $\beta_3=0.15$ for ^{106}Pd and $\beta_2=0.23$, $\beta_3=0.14$ for ^{108}Pd . These values are consistent with the older Coulomb excitation studies [4].

The octopole state was identified at 2.07 MeV in ^{106}Pd and 2.03 MeV in ^{108}Pd . The differential cross sections of the two quadrupole phonon states have been compared with CC calculations by Tamura. To achieve agreement between experiment and theory these authors find in studying the second 2^+ level that it was necessary to admix the one - and two - quadrupole phonon states. Similar investigations for ^{110}Pd have been performed with the aim to identify levels below 3 MeV and extract the deformation parameters $\beta_2=0.241$, $\beta_3=0.134$. The 3^- state was positioned at 2.038 MeV. CC theory was applied in the analysis of two and three phonon states and an otherwise similar philosophy than in the above mentioned work on $^{106,108}\text{Pd}$. A more recent experiment [5] uses 51.93 MeV protons to study the same isotopes with an equivalent theoretical input in DW and CC calculations. A reanalysis of these experimental proton scattering data is performed by a strong coupling approach using the coupled-channel code ECIS. This takes into account explicitly the higher-order coupling terms which are of particular interest if the first - order terms are inhibited by structure effects, as in the case of the excitation of two-phonon states. Both nuclear potential components - real and imaginary - and Coulomb potential were deformed. The corresponding deformation parameters were taken to be equal. The calculation were done within the framework of the second - order anharmonic vibrator model which takes into account the observed anharmonicities in a very simple way [6]. In the pure phonon picture the transition to a two-phonon state is forbidden in the first order. The population of two-phonon states can only occur in first order through anharmonic terms in the vibrational interaction, or in multi-step transitions via an intermediate

one-phonon state. The quadrupole two-phonon states with spins $I = 2^+, 4^+$ have some one-phonon admixture with multipolarity I ; thus the first order term in the coupling has a non vanishing reduced matrix element. Due to the interference between the one- and two-step transitions the scattering angular distribution corresponding to a two-phonon state is rather sensitive to the one-phonon admixture namely to the sign and magnitude of the amplitude of the admixed one-phonon component.

The optical potentials used in our calculations were fixed at the parameter values given in Refs. 2,3 and 6. The 25 MeV and 40 MeV predictions were obtained using Bechetti and Greenless parameters [7]. The differential cross sections (Fig. 1) of elastic scattering were calculated using a simple coupling scheme $O_1^+ - 2_1^+ - 3_1^-$. The same scheme was used to calculate the angular distributions of the inelastic scattering leading to the quadrupole and octopole one-phonon states, Figs. 2-5. The quadrupole excitation of the one-phonon 2_1^+ state and the $2_2^+, 4_1^+, O_2^+$ members of the two-phonon triads were investigated coupling the $O_1^+ - 2_1^+ - O_2^+ - 2_2^+ - 4_1^+$ states. The inelastic scattering cross sections are shown in Figs. 8,9 and Figs. 10,11 for 13 MeV and 52 MeV scattering from ^{106}Pd , ^{108}Pd and ^{110}Pd respectively. Unfortunately, the experimental O^+ and 2^+ or O^+ and 4^+ differential cross sections cannot be separated; the sum was available for the analysis. However, concerning the angular distributions for the separated two-phonon states there are no obvious phase relations to those in elastic scattering. This is an important indication for interferences between the one- and two-step transitions.

The predictions, Figs. 12,13, for 40 MeV are obtained from CC calculation using the deformation parameters extracted from experimental data in our above analysis. The same coupling schemes were applied as in the 53 MeV calculation. More recent investigations of the quadrupole moments in $^{102-110}\text{Pd}$ can be found in Refs. 8-11.

3. COUPLED CHANNEL ANALYSIS INVOLVING THE GIANT RESONANCE REGION

In light to medium weight nuclei elastic and inelastic scattering data are often burdened with a peak in the large angle scattering region. The peak cannot be explained with the standard optical potential choice. In recent years many attempts have been made on the basis of shell effects [12], multistep processes, intermediate deuteron coupling [13], ℓ -dependent optical potentials [14] etc. to clarify the failures of the OMP.

Machintosh and Robers obtain fits of high quality to proton elastic scattering from nuclei with masses from 16 to 58 over a wide range of energies using a local optical model and the addition of explicitly ℓ -dependent real and imaginary terms. The general characteristics of these terms were related to the fact that channel coupling introduces ℓ -dependent effects. The above mentioned authors ascertain reaction channels as prevailing.

At present it seems not anymore doubtful that an ℓ -dependent small modification of OMP phase shifts $\ell \leq 6$, is required to obtain fits to data. The different approaches of Refs. 12,13 and 14 have the bad flavour to reply on many ad hoc introduced parameters.

In a recent theoretical investigation [15] mainly on ^{40}Ca data, we found giant resonances are primarily responsible. Giant resonances (here we mean the GDR and GQR) in light to medium weight nuclei are spread over a wide energy range with no major concentration in one single state. This is not so for heavier nuclei where the GQR can be well allocated at $63/A^{1/3}$ with a width of 3-5 MeV and a strength exhausting 50-100% of the EWSR. In the scattering experiments from ^{144}Sm in an energy range 15 to 25 MeV similar anomalies of the elastic and inelastic large angle scattering has been detected as for the mentioned light to medium weight nuclei [15]. The effect, however, is less pronounced.

With the scattering experiments on Palladium isotopes it occurs suitable to incorporate studies of giant resonance coupling with the ground state and the low lying vibrational spectrums.

In the scattering experiments from ^{144}Sm in an energy range 15 to 25 MeV similar anomalies of elastic and inelastic large angle scattering has been detected as for the mentioned light to medium weight nuclei [15] the effect however, is less pronounced.

With the scattering experiments on Palladium isotopes it occurs suitable to incorporate studies of giant resonance coupling with the ground state and the low lying vibrational spectrum. The influence of the GQR at 13.5 MeV on the elastic channel for various strengths $\beta_2 = 0(0\%); 0,146(100\%); 0,29(400\%)$ in relativ units of the EWSR are investigated. The changes are modest in structure even at large scattering angles. In the energy region between 13 and 25 MeV a shift of the diffraction minima can be seen. In this effect which we would like to identify with the light precision measurements of the elastic channel cross section.

As condition for the measurements we have therefore to impose severe care when taking data with respect to many possible systematic errors or contaminations of the targets the relative accuracy of angular distribution should be less than 1% and the absolute normalization not wronger than 5%.

In view of the wide isotope range it might appear suitable to design appropriate experimental techniques to obtain high precision relative angular distributions [17]. Such data could be of great value for the microscopic analyses.

Regarding the smallness of the coupling effect to the GQR the experimental data and the therefrom derived conclusions in Ref.16 seems doubtful.

4. MICROSCOPIC OPTICAL POTENTIALS

The nucleon nucleus optical potential is based on the two nucleon t -matrix calculated in nuclear matter for different densities and incident projectile energies [18]. For convenience it is represented by a local density and energy dependent potential in coordinate space; viz.

$$t = \sum_{ST} t^{ST}(r, k_F, E),$$

where

$$\rho = \frac{2}{3\pi^2} k_F^3,$$

with numerically tabulated values for t^{ST} [19]. The indices S and T refer to the two nucleon relative spin and isospin.

The next procedure assumes that at each point in a finite nucleus the value of the OMP is well approximated with the OMP of infinitely extended nuclear matter calculated with the local quantum numbers. This rather crude model is generally referred to as "local density approximation" (LDA).

Another improved version of the finite nucleus OMP is obtained when starting from the general formulation of the folding model. It yields in lowest order a nonlocal in r - space and energy dependent potential

$$\begin{aligned} U(\vec{r}, \vec{r}'; E) = & \delta(\vec{r} - \vec{r}') \int d^3r'' \sum_n \phi_n^*(\vec{r}'') \phi_n(\vec{r}'') \\ & \times t^D(|\vec{r}' - r''|, k_F(r''); E(r')) + \\ & + \sum_n \phi_n(r) t^{EX}(|\vec{r} - \vec{r}'|, k_F(r'); E(r')) \phi_n^*(r'). \end{aligned}$$

It contains real and imaginary parts arising from the complex valued $t(r, k_F, E)$ with a local direct terms and a nonlocal exchange term.

Recoil effect are included. The diagonal and mixed single particle density in the above expression is generated from a nonlocal single particle potential

$$\begin{aligned} V(r, r') = & V_0 [(1 + \exp(r-R)/a) (1 + \exp(r'-R)/a)]^{-1/2} \\ & \times \left(\frac{\gamma}{2\pi} \right)^{3/2} e^{-\gamma |\vec{r} - \vec{r}'|^2}. \end{aligned}$$

Fig. 14 shows the diagonal proton and neutron densities of ^{110}Pd .

A multipole decomposition of the $U(\vec{r}, \vec{r}', E)$ facilitates partial wave decomposition of the solution in the well known manner. As shown in another contribution to this volume, the practitioner equivalent local potential may be expressed by the regular and irregular solutions to the Schroedinger integrodifferential equation. We limited the calculations to $l = 0$ since the essential l -dependence of the here defined optical model has been numerically verified in ^{40}Ca . Results shown in Fig. 15, 16 display the local direct

OMP (U_D), the exchange potential, the equivalent local exchange potential, $U_{EXC} = U_{TOT} - U_D$, and the Perey effect in their radial dependence. The strong repulsive nature of U_D arises from the odd state contributions which are highly compensated by its exchange partners. The dashed curve is a phenomenological Woods-Saxon potential from the compilation of Perey/Perey. The energy dependence is shown in *Fig. 17* for three different energies for which experiments are anticipated. The ^{110}Pd results are quite typical for all Pd isotopes.

The Perey effect, $A(r)$, is a result of the r -dependence of the Wronskian for integrodifferential equations. It relates the amplitudes of the local and nonlocal wave functions

$$\psi_{NL}^{(lj)}(r) = A^{(lj)}(r) \psi_L^{(lj)}(r).$$

The expression for $A(r)$ is like the equivalent OMP essentially l -independent and is well approximated by the expression by Perey and Buck

$$A(r) = \left[1 - \frac{1}{4\gamma} \frac{2m}{\hbar^2} U_L(r) \right]^{-1/2}$$

with $\gamma = 0.8 \text{ fm}^{-2}$. The results remain valid for higher partial waves. The imaginary potential and spin-orbit potential are predominantly local and their features remain analyzed in older investigations.

REFERENCES

- [1] F. Bertrand, *Ann. Rev. Nucl. Sci.* 26 (1976) 457
- [2] R.L. Robinson et al., *Phys. Rev.* 146 (1966) 816
- [3] R.L. Robinson et al., *Phys. Rev.* 189 (1968) 1609
- [4] R.L. Robinson et al., *Nucl. Phys.* A129 (1968) 553
- [5] M. Koike et al., *Nucl. Phys.* A248 (1975) 237
- [6] T. Tamura, *Supp. Prog. Theor. Phys.* 37/38 (1966) 383
- [7] F.B. Becchetti and G.N. Greenles, *Ann. Rep.* (1968) Univ. of Minnest
- [8] M. Maynard et al., *J. Phys. G. Nucl. Phys.* 3 (1977) 1735
- [9] R.G. Arthur et al., *J. Phys. G. Nucl. Phys.* 4 (1978) 961
- [10] J. Lange et al., *Nucl. Phys.* A292 (1977) 301
- [11] J.W. Lightbody et al., *Phys. Rev.* 14 (1976) 952
- [12] M. Pignanelly, in *Microscopic Optical Potentials*, *Lect. Notes in Physics* 89 (1979) 211
ed. H.V. von Geramb
and *Proc. of the Bormio Winterscool 1971*, Milano
ed. I. Jori
- [13] R.S. Mackintosh and A.M. Kobos, *Phys. Lett.* 62B (1976) 127
- [14] R.S. Mackintosh and L.A. Cordero, *Phys. Lett.* 68B (1977) 213
- [15] M. Pignanelli and H.V. von Geramb, to be published
- [16] R. Lisdat, *Dissertation*, Univ. Hamburg 1977
- [17] S.M. Austin, in *Microscopic Optical Potentials*, *Lect. Notes in Physics* 89 1979 239, ed. H.V. von Geramb
- [18] F.A. Brieva, *Nucl. Phys.* A291 (1977) 299, 317
- [19] H.V. von Geramb, F.A. Brieva and J.L. Rook, in *Microscopic Optical Potentials*, *Lect. Notes in Physics* 89 (1979), 104, ed. H.V. von Geramb and H.V. von Geramb, Universität Hamburg (unpublished)

Table

Summary of the potential and deformation parameters used in CC calculations

Energy MeV	Nucl.	V_O^{MeV}	W_V^{MeV}	W_{SF}^{MeV}	V_{SO}^{MeV}	r_{or}^{fm}	a_r^{fm}	r_{oi}^{fm}	a_i^{fm}	r_{os}^{fm}	a_s^{fm}	β_2	β_3	γ_2°	γ_4°
13	^{106}Pd	55.4	0.	10.35	6.	1.2	0.7	1.25	0.65	1.2	0.7	0.24	0.15	76°	60°
40		54.67	6.9	8.58	6.2	1.17	0.75	1.32	0.906	1.01	0.75	0.24	0.18	76.7°	60°
53		44.97	0.	8.67	7.15	1.19	0.69	1.19	0.8	1.2	0.69	0.24	0.18	76.7°	60°
13	^{108}Pd	55.4	0.	11.2	6.	1.2	0.7	1.25	0.65	1.2	0.7	0.25	0.15	78.4°	60°
40		54.84	6.9	8.69	6.2	1.17	0.75	1.32	0.91	1.01	0.75	0.26	0.17	79.6°	60°
53		43.96	0.	9.44	7.35	1.19	0.69	1.19	0.8	1.2	0.69	0.26	0.17	79.6°	60°
13	^{110}Pd	55.7	0.	9.42	9.65	1.2	0.7	1.25	0.65	1.2	0.7	0.28	0.14	73°	60°
40		56.01	6.9	8.78	6.2	1.17	0.75	1.32	0.91	1.01	0.75	0.28	0.14	77.8°	60°
53		41.35	0.	9.42	8.63	1.19	0.69	1.25	0.93	1.2	0.69	0.28	0.14	77.8°	60°

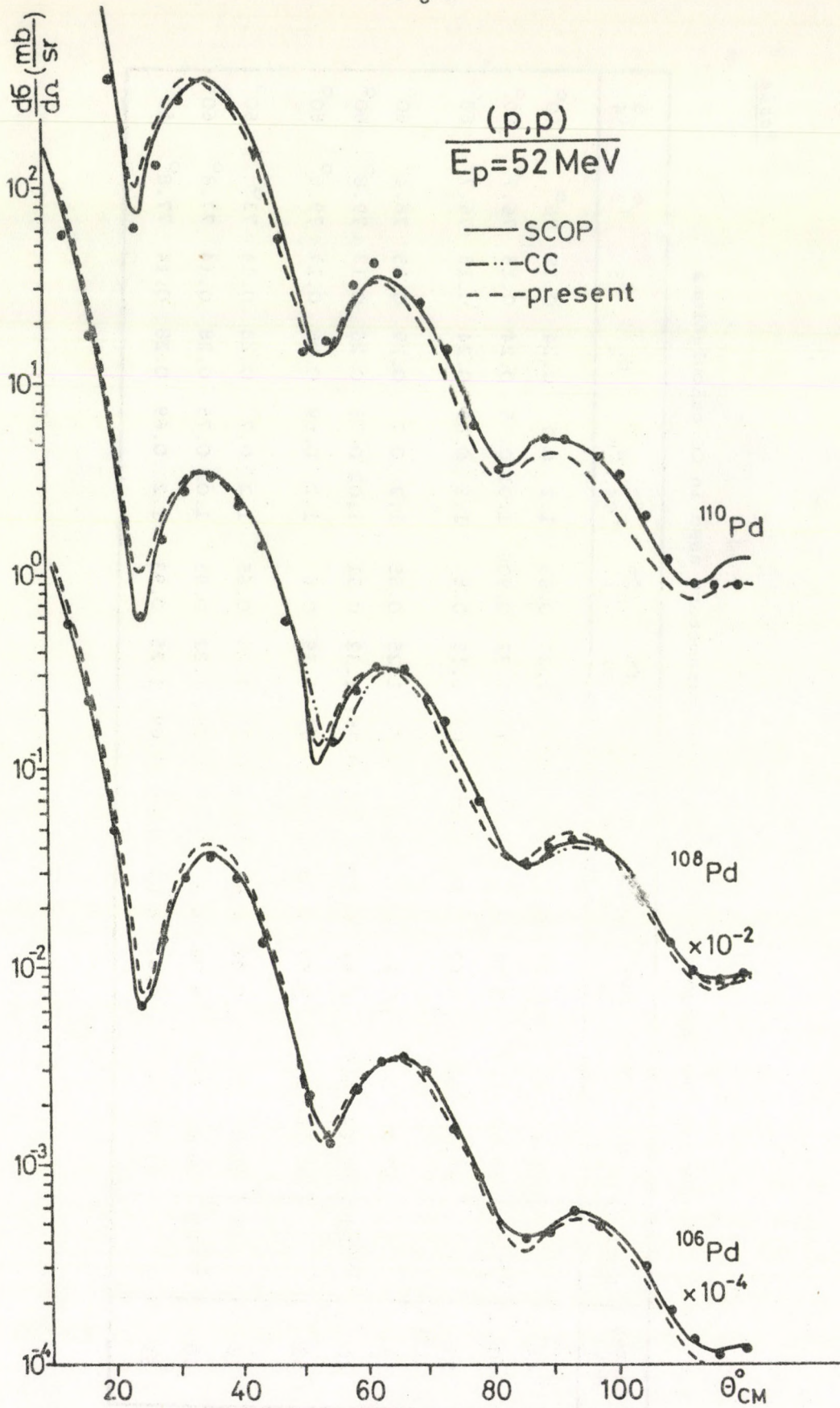


Fig. 1

Differential cross sections of elastic scattering.
Experimental data were taken from Refs. 2, 3 and 6

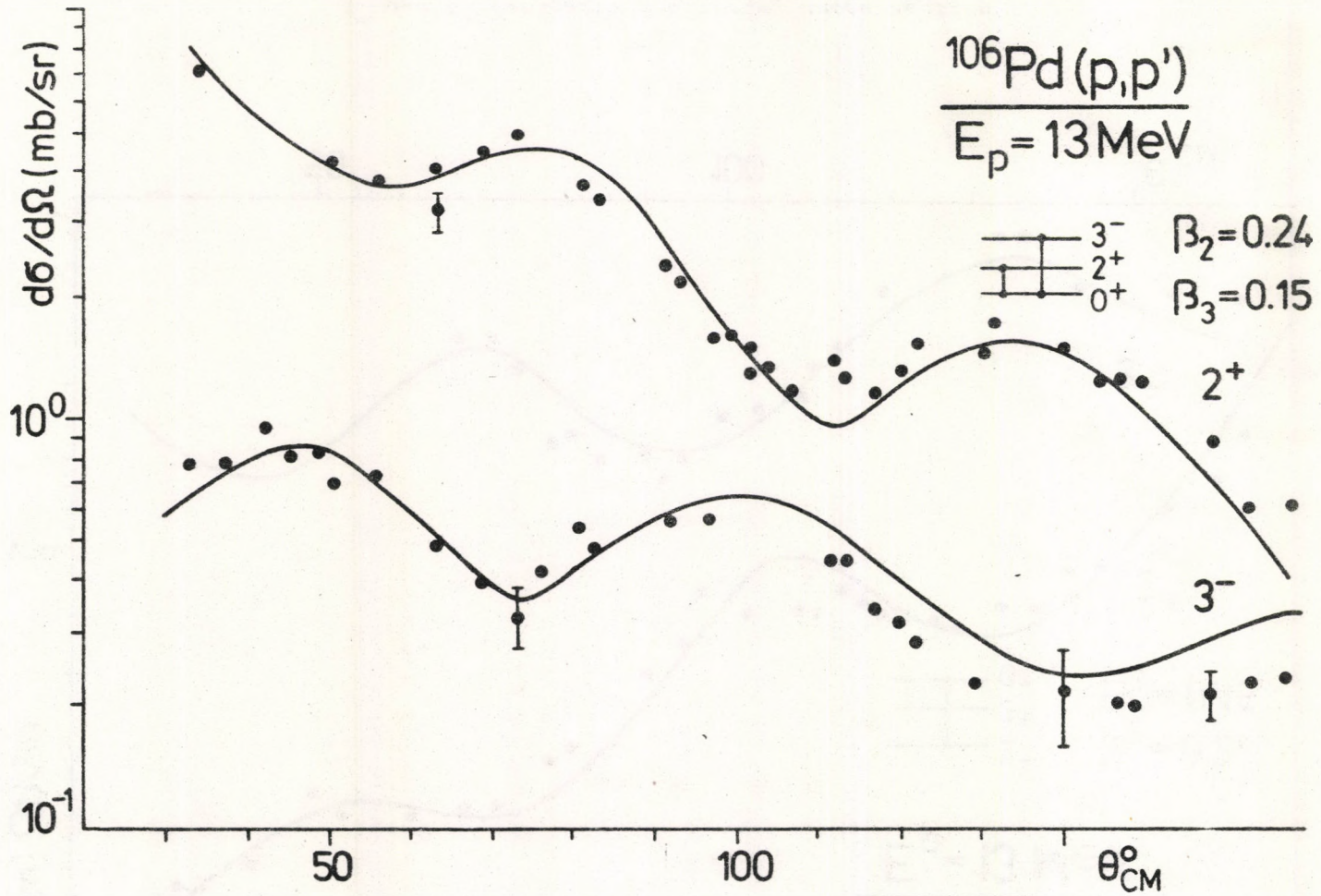


Fig. 2
 2^+ and 3^- inelastic scattering cross section
 at 13 MeV energy for ^{106}Pd nucleus

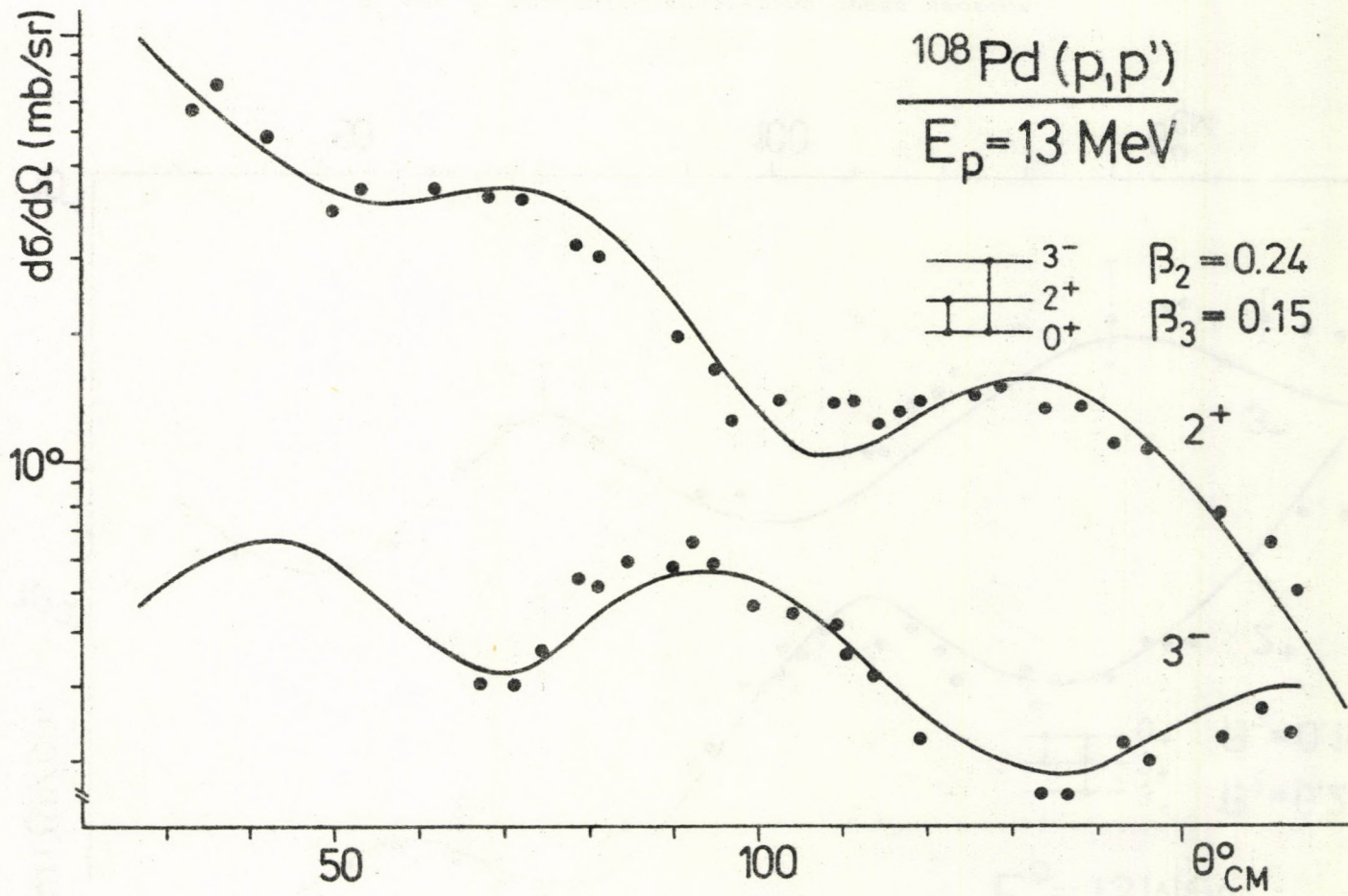


Fig. 3
2⁺ and 3⁻ inelastic scattering cross section
at 13 MeV for ^{108}Pd nucleus

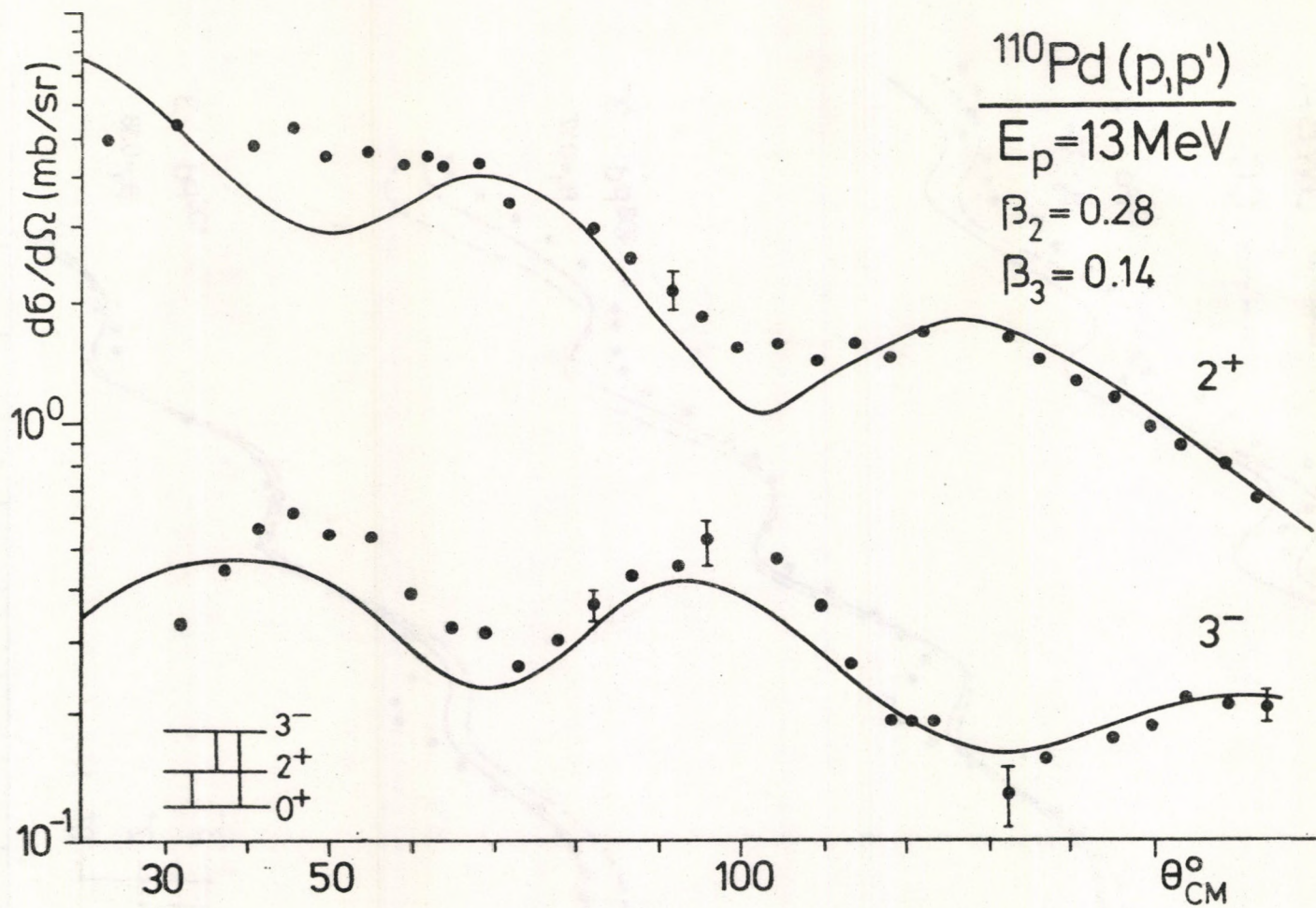


Fig. 4
 2^+ and 3^- inelastic scattering cross section
 at 13 MeV for ^{110}Pd nucleus

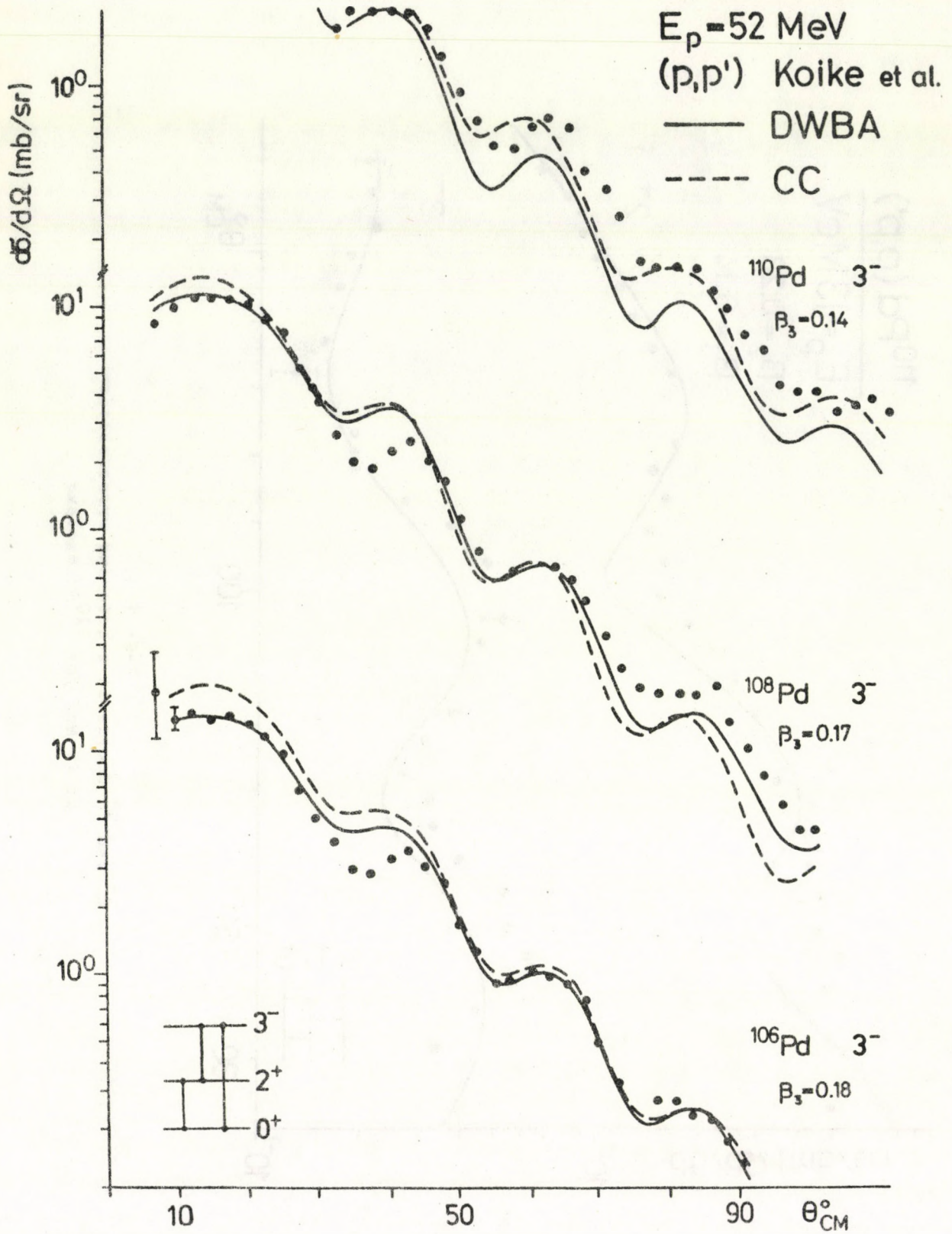


Fig. 5
 3^- inelastic scattering cross section at 52 MeV for $^{106}, ^{108}, ^{110}\text{Pd}$

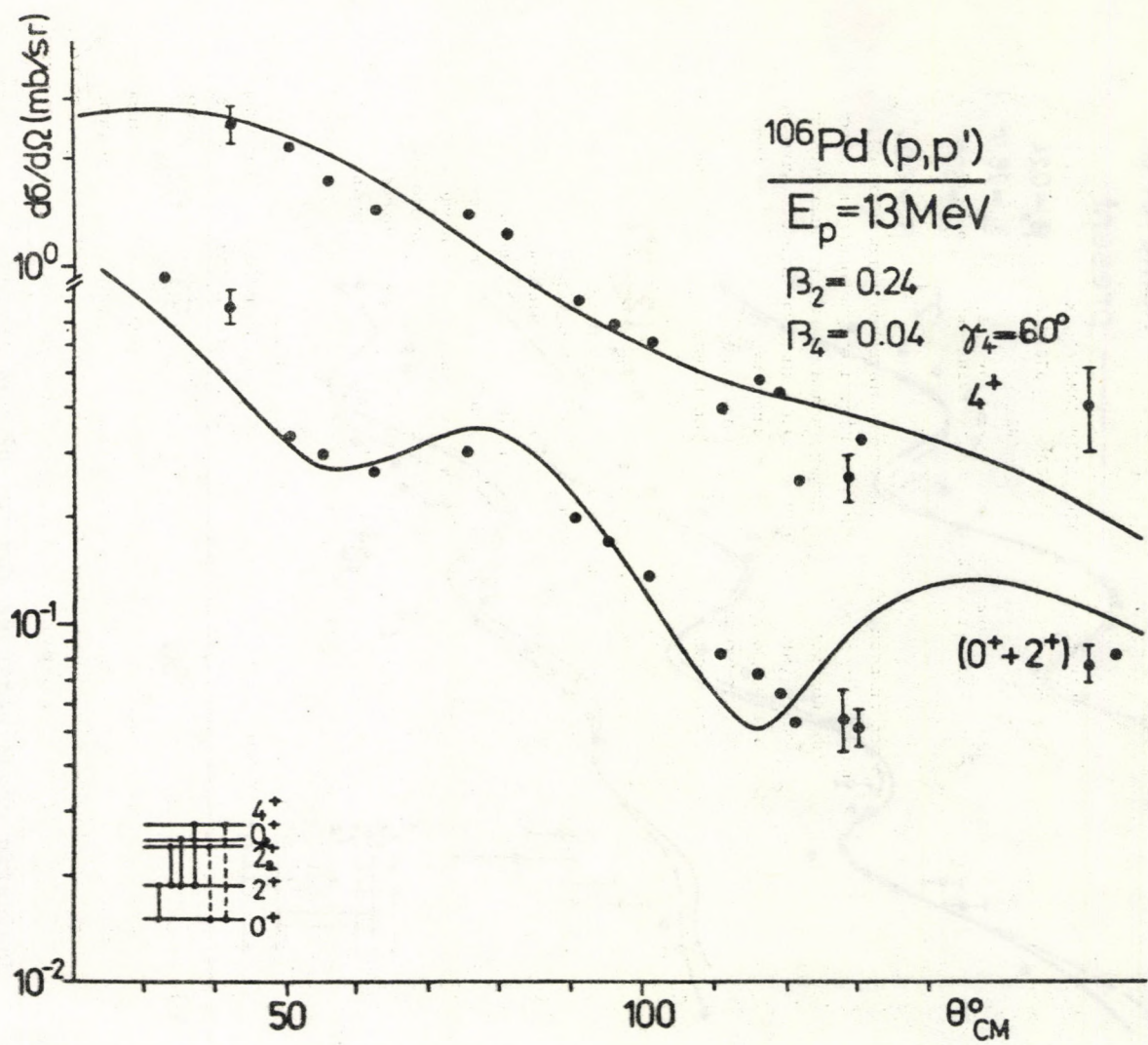


Fig. 6
 Inelastic cross section for two-phonon states in ^{106}Pd at 13 MeV

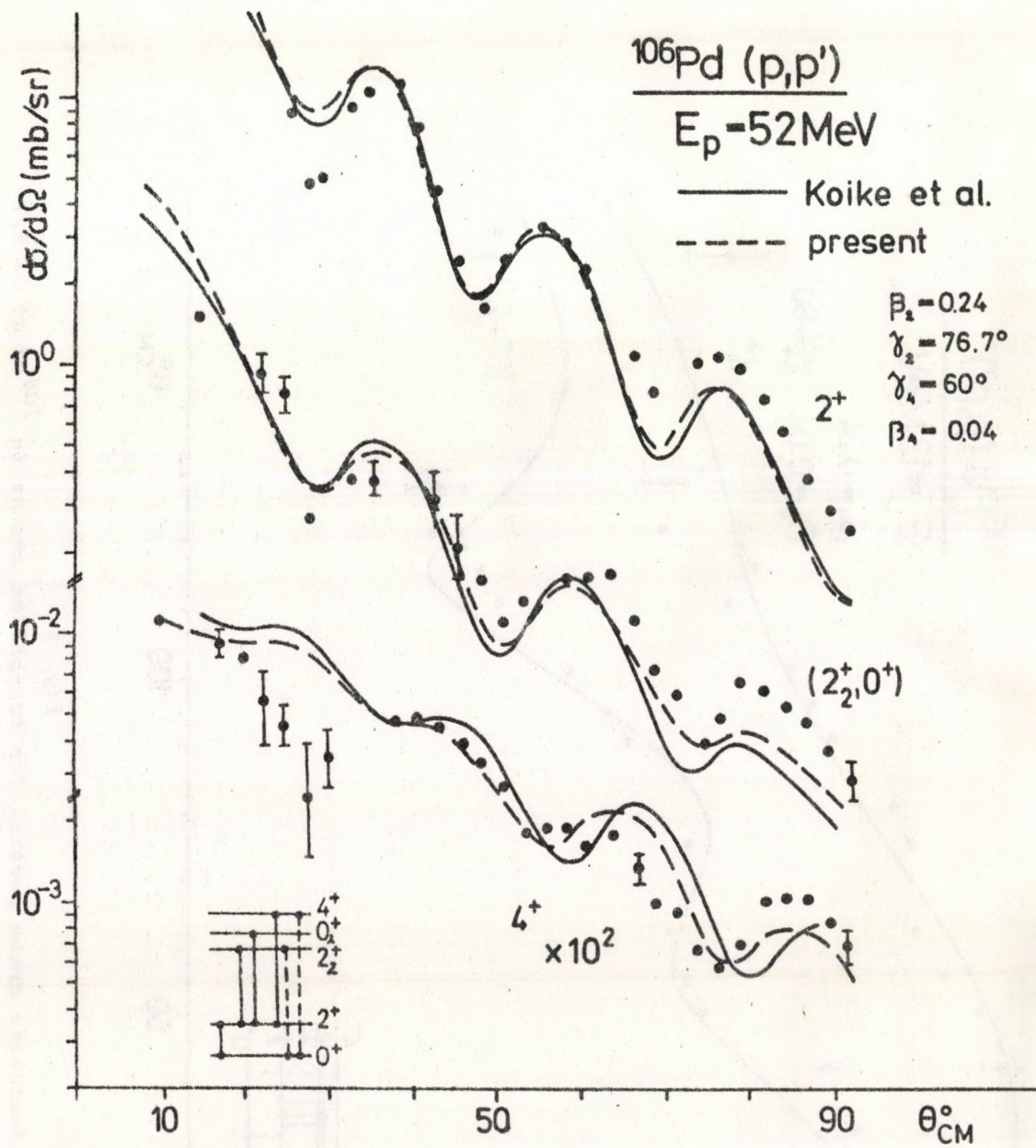


Fig. 7
Inelastic cross sections for two-phonon states
in ^{106}Pd at 52 MeV

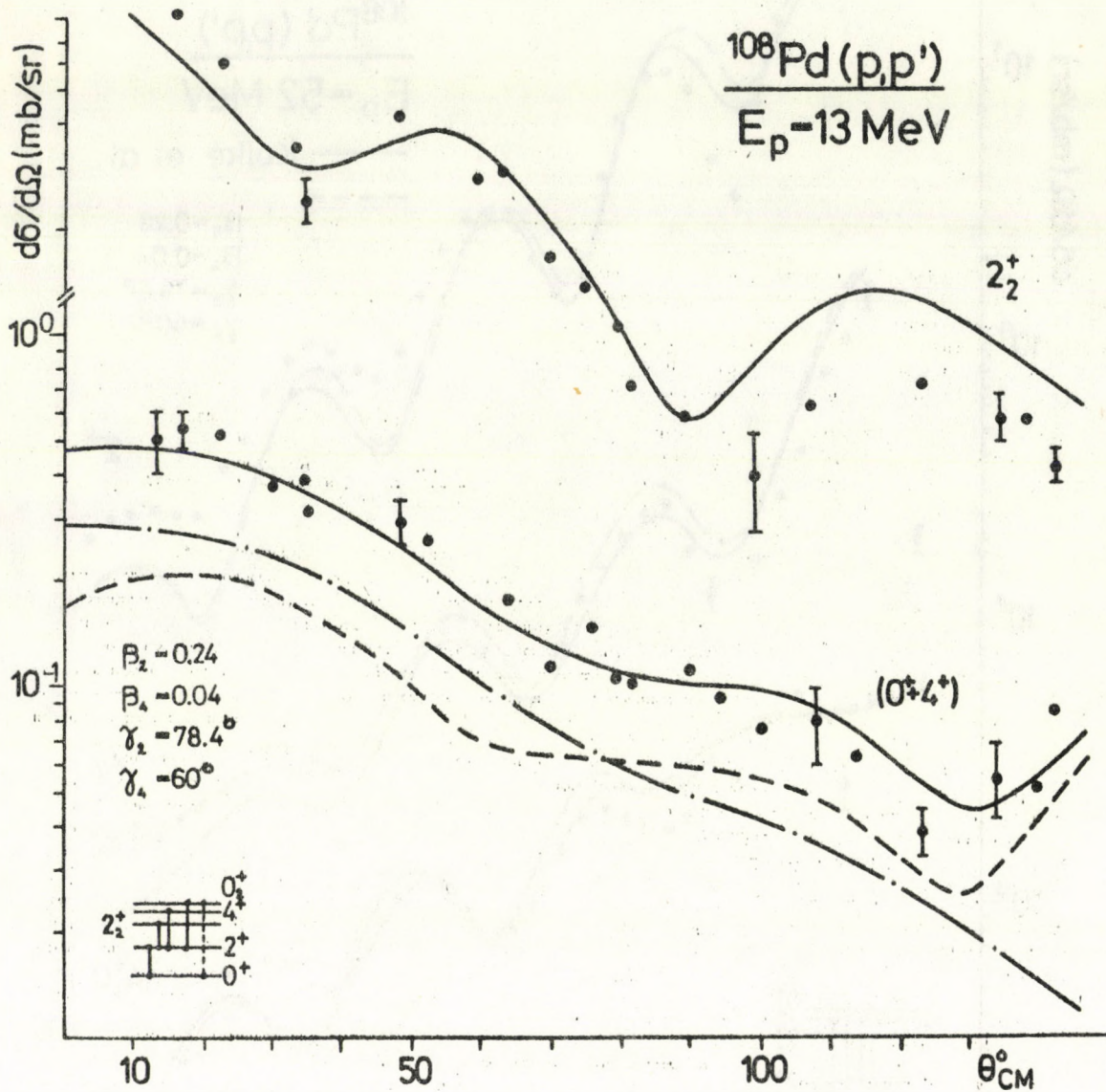


Fig. 8
Inelastic cross sections for two-phonon states
in ^{108}Pd at 13 MeV

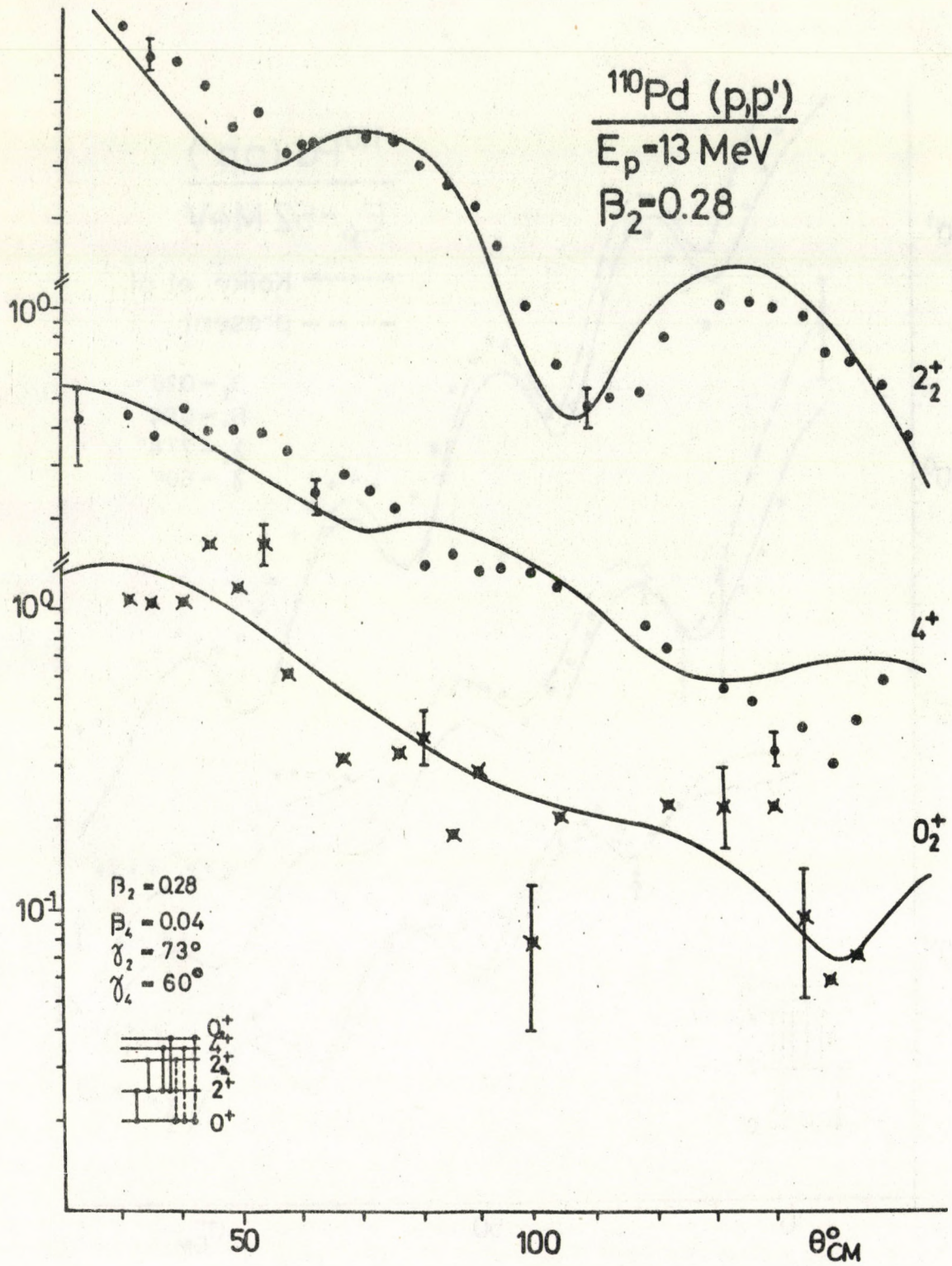


Fig. 10
Inelastic cross sections for two-phonon states
in ^{110}Pd at 13 MeV

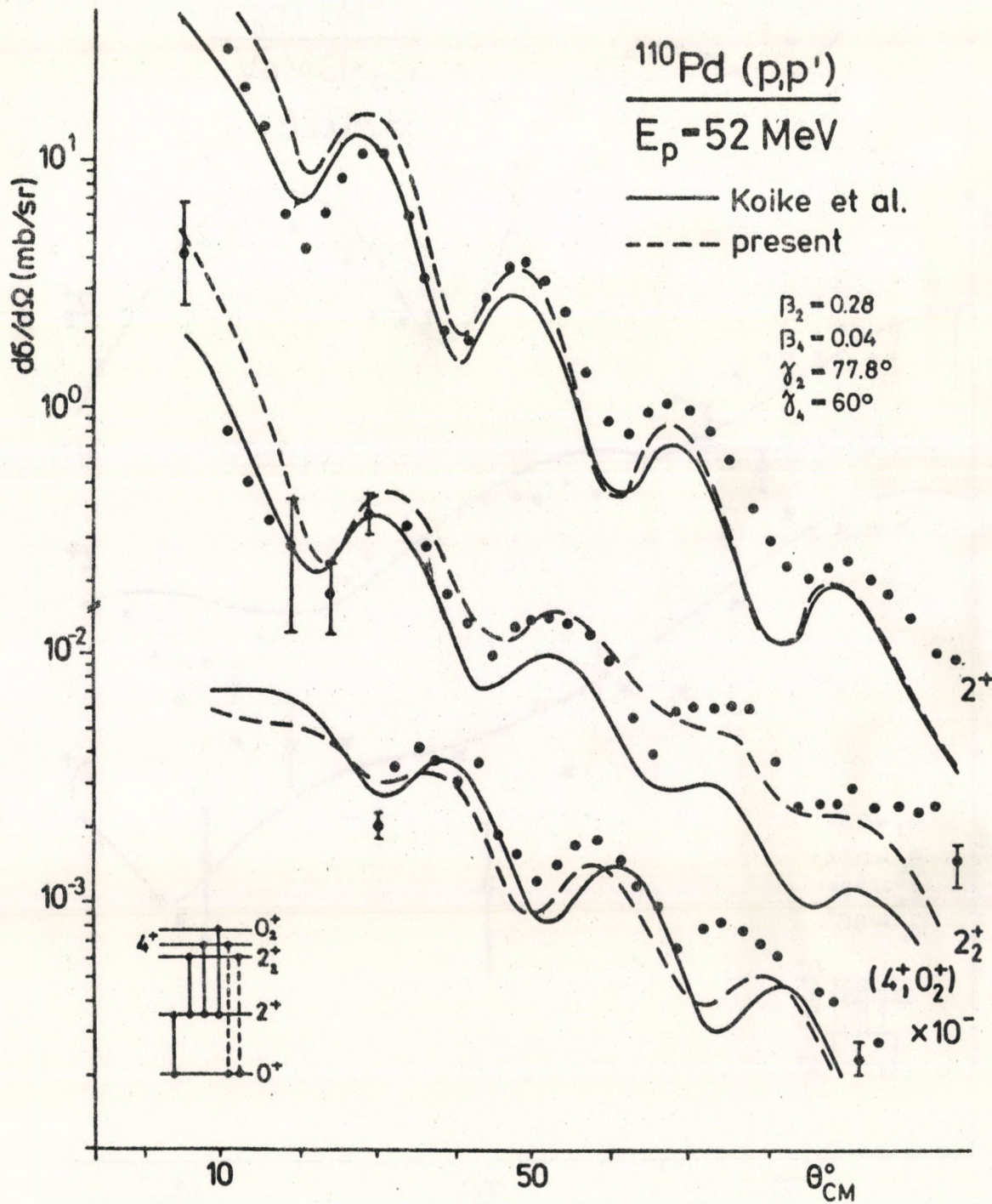


Fig. 11
 Inelastic cross sections for two-phonon states
 in ^{110}Pd at 52 MeV

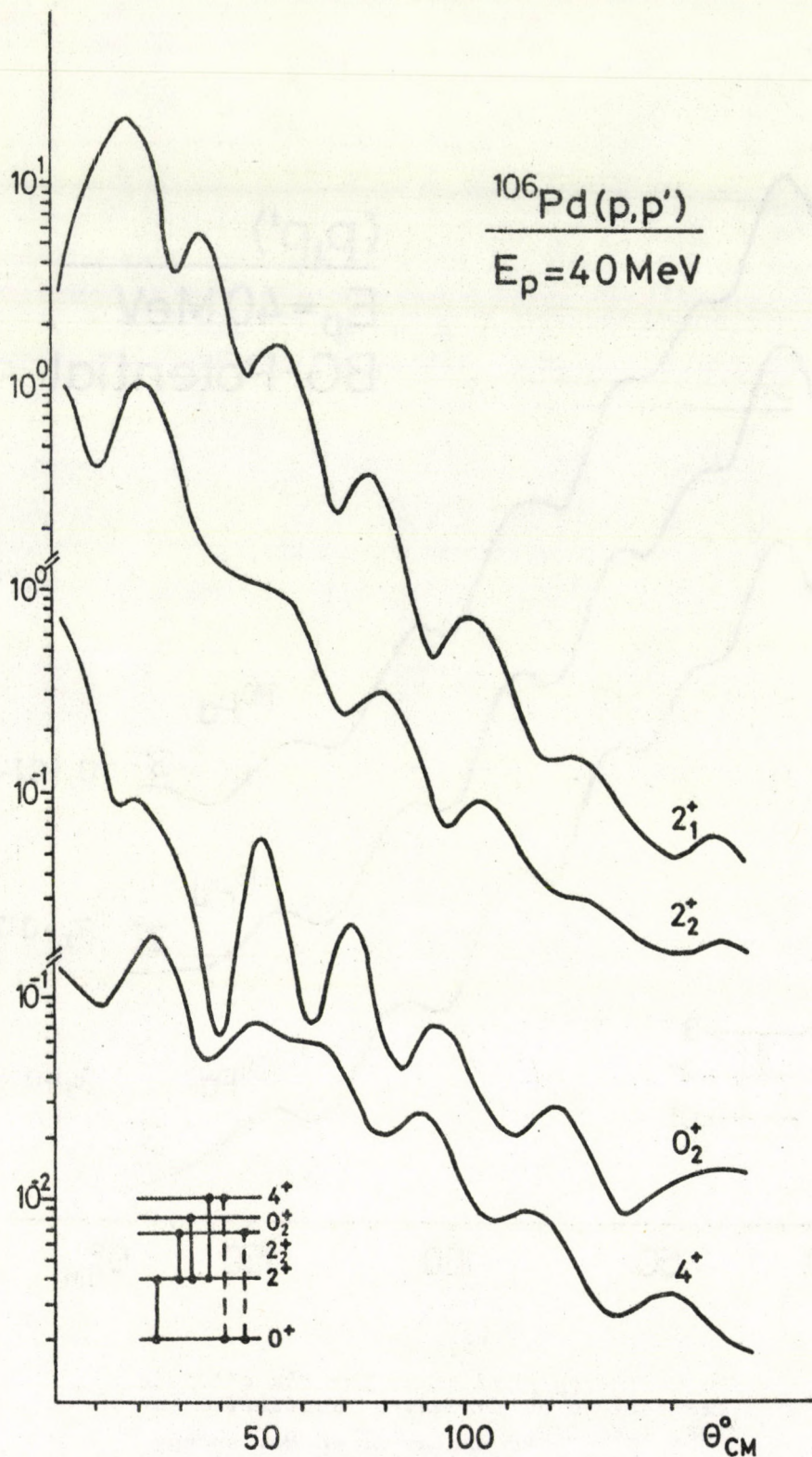


Fig. 12

The CC-theory prediction for the two-phonon excitation by inelastic scattering in ^{106}Pd at 40 MeV energy

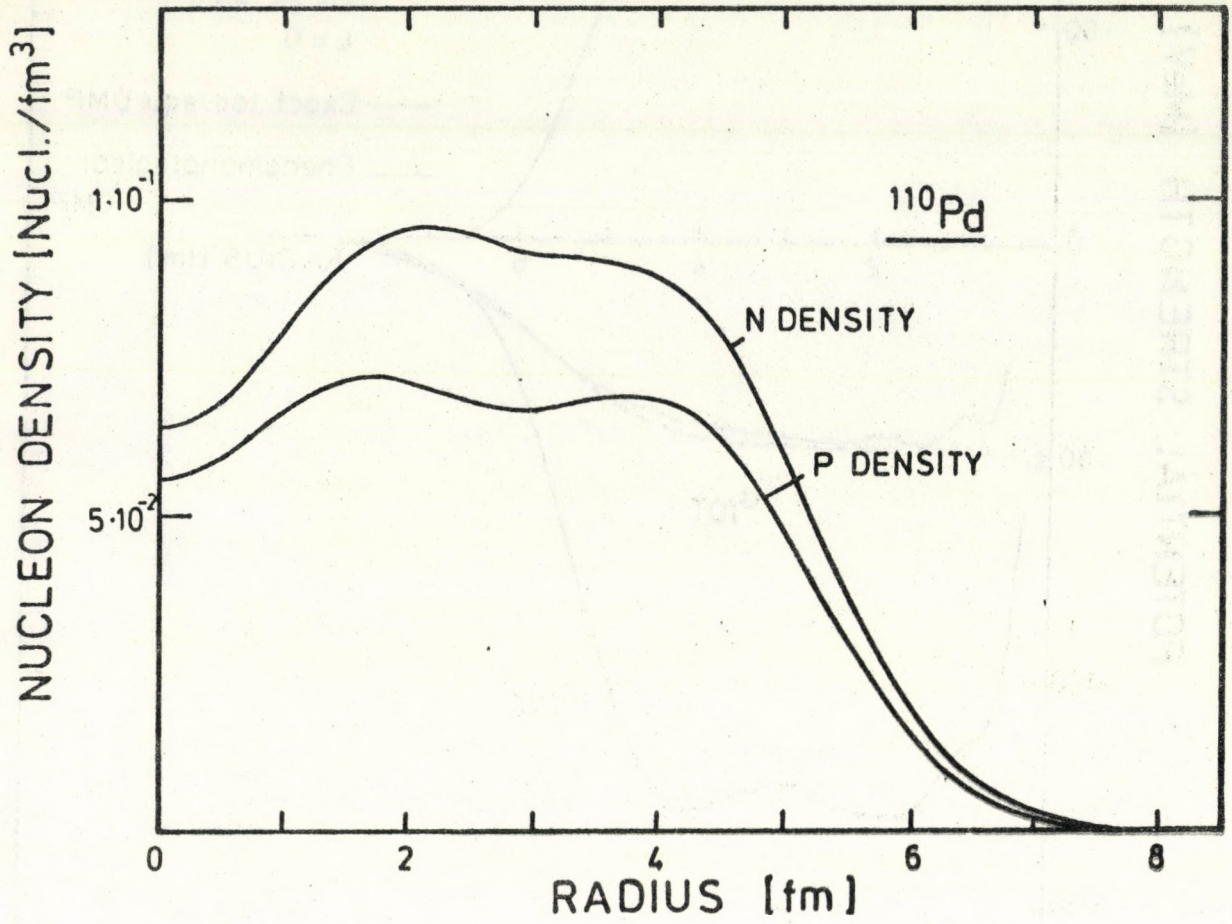


Fig. 14
Diagonal proton and neutron densities of
 ^{110}Pd nucleus

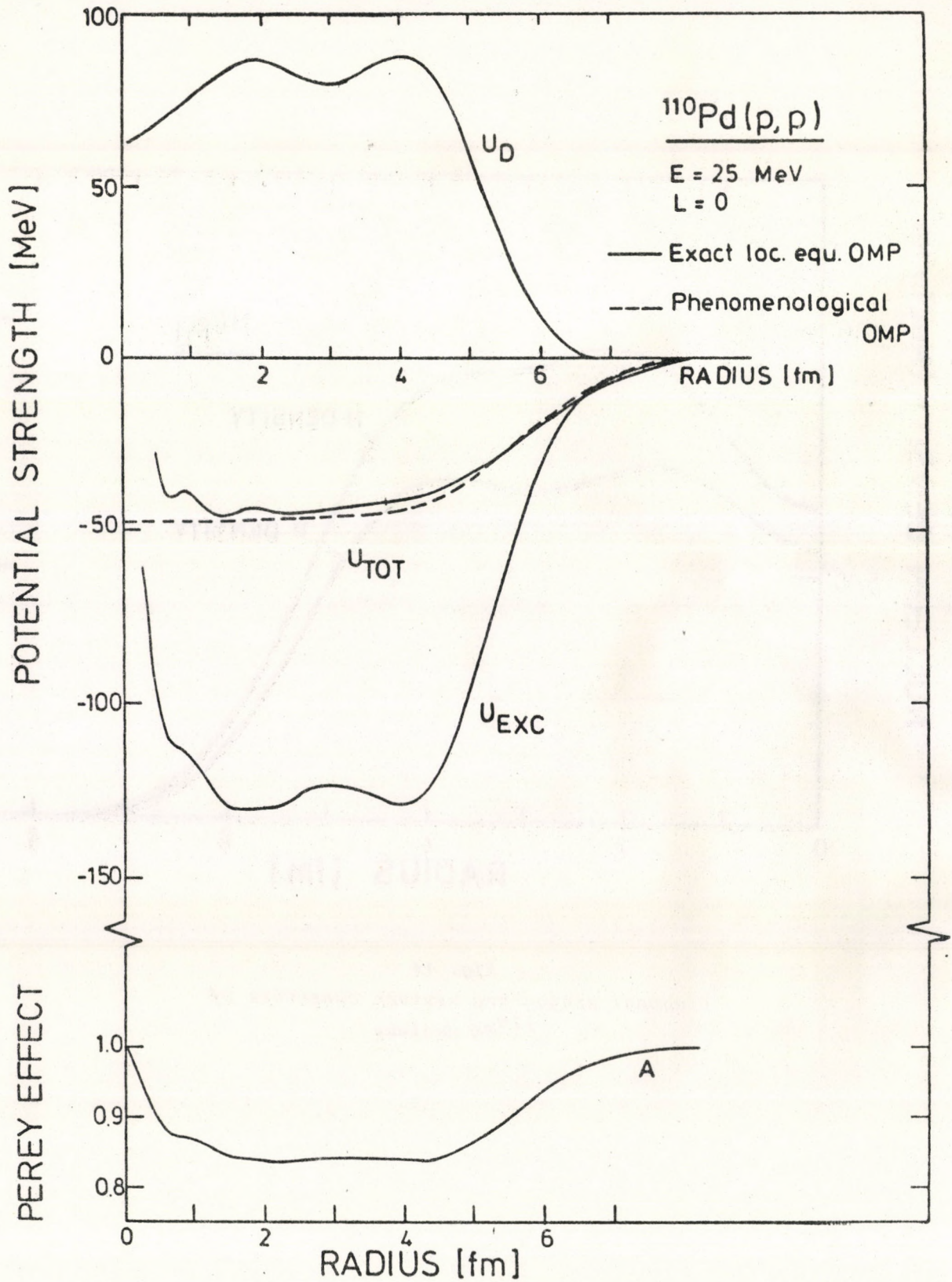


Fig. 15
Local equivalent optical potential for ^{110}Pd nucleus

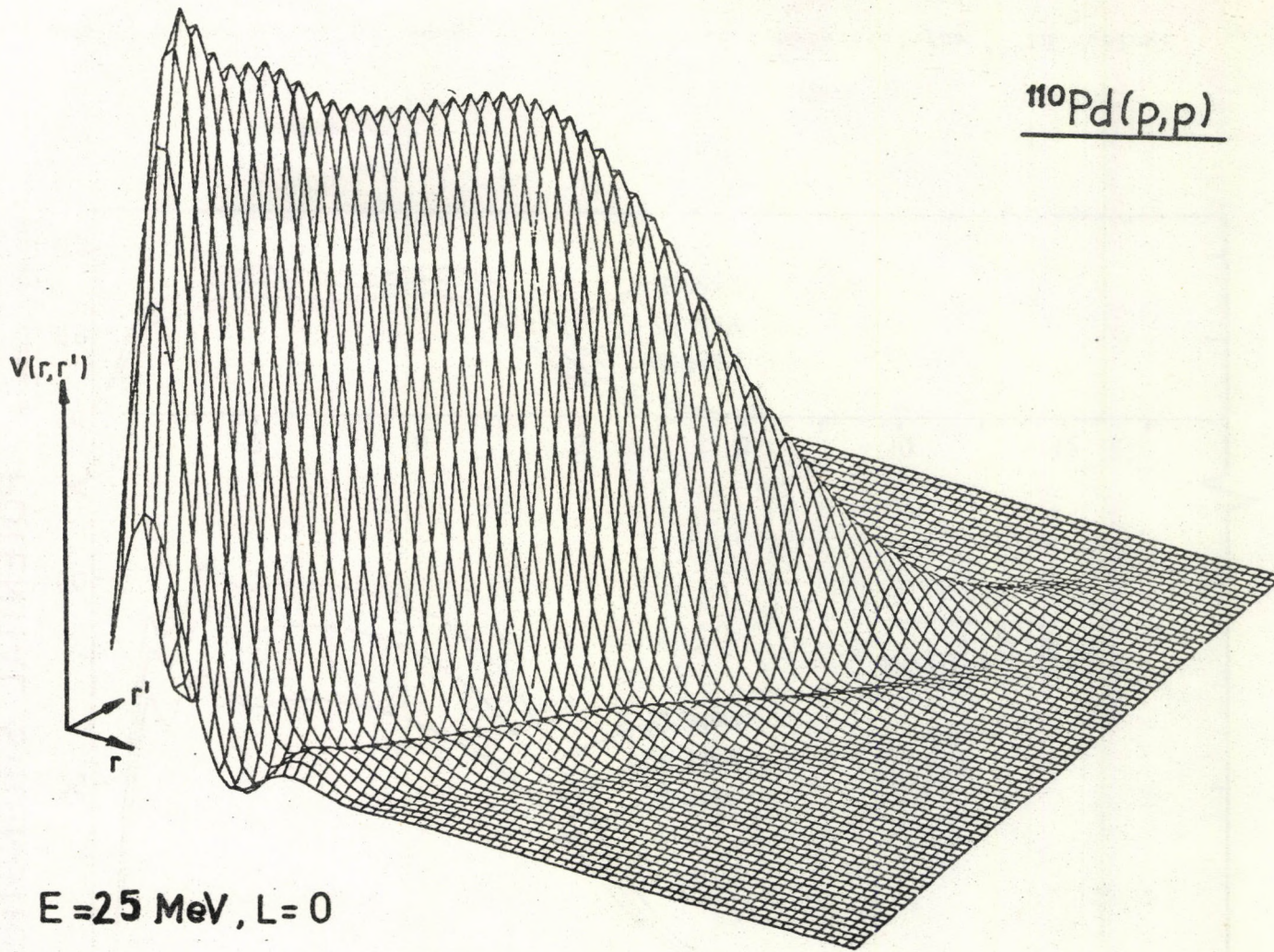


Fig. 16
Exchange potential kernel for ^{110}Pd nucleus

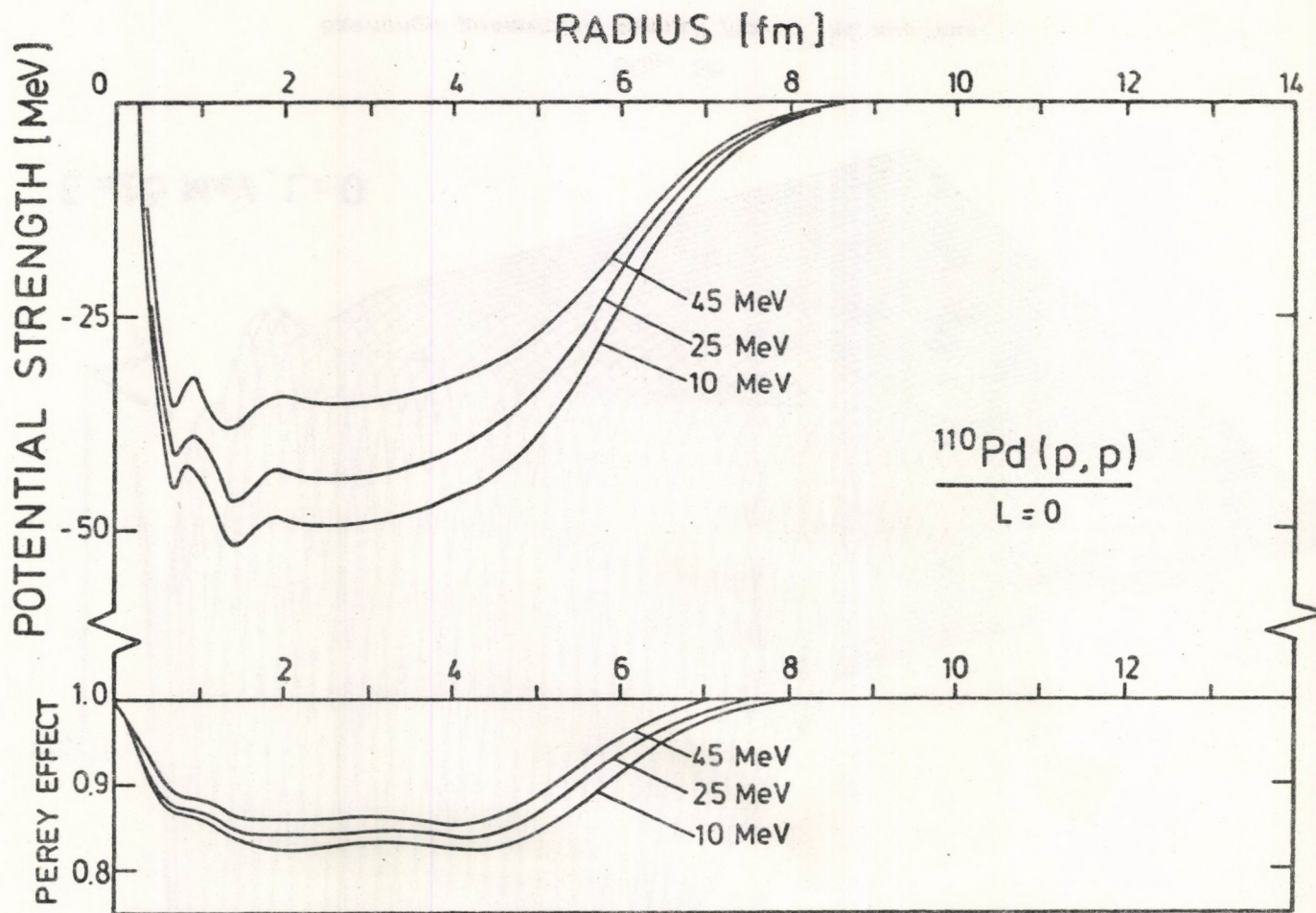


Fig. 17
 Energie-dependence of the local equivalent optical potential for ^{110}Pd nucleus







Kiadja a Központi Fizikai Kutató Intézet
Felelős kiadó: Szegő Károly
Szakmai lektor: Doleschall Pál
Nyelvi lektor: Révai János
Példányszám: 170 Törzsszám: 80-234
Készült a KFKI sokszorosító üzemében
Budapest, 1980. május hó